⌘ *Author's Choice*

THE JOURNAL OF BIOLOGICAL CHEMISTRY VOL. 286, NO. 42, pp. 36448–36459, October 21, 2011

Local Cytosolic Ca^{2+} Elevations Are Required for Stromal Interaction Molecule 1 (STIM1) De-oligomerization and Termination of Store-operated Ca^{2+} Entry*[S]

Received for publication, June 10, 2011, and in revised form, August 12, 2011 Published, JBC Papers in Press, August 31, 2011, DOI 10.1074/jbc.M111.269415

Wei-Wei Shen, Maud Frieden, and Nicolas Demaurex[1]

From the Department of Cell Physiology and Metabolism, University of Geneva, rue Michel-Servet 1, CH-1211 Geneva 4, Switzerland

Background: STIM1 oligomerization upon endoplasmic reticulum (ER) Ca^{2+} depletion activates store-operated Ca^{2+} entry (SOCE) channels, but whether this mechanism is reversible is unknown.
Results: STIM1 de-oligomerization upon ER Ca^{2+} refilling requires concomitant cytosolic Ca^{2+} elevations near STIM1 membrane clusters.
Conclusion: Cytosolic Ca^{2+} elevations dissociate STIM1 oligomers during SOCE termination.
Significance: Ca^{2+} acts on a cytosolic target to control the disassembly of STIM1 membrane clusters.

The Ca^{2+} depletion of the endoplasmic reticulum (ER) activates the ubiquitous store-operated Ca^{2+} entry (SOCE) pathway that sustains long-term Ca^{2+} signals critical for cellular functions. ER Ca^{2+} depletion initiates the oligomerization of stromal interaction molecules (STIM) that control SOCE activation, but whether ER Ca^{2+} refilling controls STIM de-oligomerization and SOCE termination is not known. Here, we correlate the changes in free luminal ER Ca^{2+} concentrations ($[Ca^{2+}]_{ER}$) and in STIM1 oligomerization, using fluorescence resonance energy transfer (FRET) between CFP-STIM1 and YFP-STIM1. We observed that STIM1 de-oligomerized at much lower $[Ca^{2+}]_{ER}$ levels during store refilling than it oligomerized during store depletion. We then refilled ER stores without adding exogenous Ca^{2+} using a membrane-permeable Ca^{2+} chelator to provide a large reservoir of buffered Ca^{2+}. This procedure rapidly restored pre-stimulatory $[Ca^{2+}]_{ER}$ levels but did not trigger STIM1 de-oligomerization, the FRET signals remaining elevated as long as the external $[Ca^{2+}]$ remained low. STIM1 dissociation evoked by Ca^{2+} readmission was prevented by SOC channel inhibition and was associated with cytosolic Ca^{2+} elevations restricted to STIM1 puncta, indicating that Ca^{2+} acts on a cytosolic target close to STIM1 clusters. These data indicate that the refilling of ER Ca^{2+} stores is not sufficient to induce STIM1 de-oligomerization and that localized Ca^{2+} elevations in the vicinity of assembled SOCE complexes are required for the termination of SOCE.

Store-operated Ca^{2+} entry (SOCE)[2] is a cellular mechanism that couples the Ca^{2+} depletion of the endoplasmic reticulum (ER) to the activation of plasma membrane Ca^{2+}-permeable channels (1). SOCE is required for the generation of the sustained Ca^{2+} signals that mediate secretion, metabolism, and proliferation in both excitable and nonexcitable cells (2), and disruptions in the SOCE pathway lead to severe immune disorders (3–6) and to altered function of skeletal and smooth muscle cells as well as endothelial cells (5, 7–9). The concept that Ca^{2+} depletion of the ER activates membrane channels was proposed 25 years ago (10), but the molecules that mediate this process were unveiled only in 2005. Two families of proteins were identified by genome wide interfering RNA screens: the stromal interaction molecules (STIM), ER transmembrane proteins that sense the Ca^{2+} filling state of the ER to control SOCE (11, 12), and the plasma membrane-spanning proteins Orai1, Orai2, and Orai3 (13–15) that are the pore-forming subunits of SOCE channels.

STIM1 and its homologue STIM2 are single pass type I ER transmembrane proteins bearing a luminal EF-hand Ca^{2+}-binding motif fused to a sterile α motif (SAM), and a cytosolic tail containing two proximal coiled-coiled domains and a terminal lysine-rich domain. Ca^{2+} unbinding from the EF-SAM domain (STIM1: K_d 0.2–0.6 mM (16)) induces STIM1 oligomerization and exposes interacting domains in the STIM1 cytosolic tail that bind to the C terminus of Orai channels and induce their activation (17–20). A region of 100 amino acids containing the STIM1 second coiled-coil domain, the CRAC (Ca^{2+} release-activated Ca^{2+} current) activation domain (CAD), also known as the STIM-Orai activating region or Orai1-activating small fragment, is sufficient to activate Orai channels (17–19, 21). In resting cells, the high free Ca^{2+} concentration within the ER lumen ($[Ca^{2+}]_{ER}$) of 300–600 μM (22) stabilizes the protein in an inactive state via intra-molecular

* This work was supported by Swiss National Foundation Grant 310030B-133126 (to N. D.).
⌘ *Author's Choice*—Final version full access.
[S] The on-line version of this article (available at http://www.jbc.org) contains supplemental Figs. S1–S4.
[1] To whom correspondence should be addressed. Tel.: 41-22-379-5399; Fax: 41-22-379-5338; E-mail: Nicolas.Demaurex@unige.ch.
[2] The abbreviations used are: SOCE, store-operated Ca^{2+} entry; BAPTA-AM, 1,2-bis(*o*-aminophenoxy)ethane-*N*,*N*,*N*′,*N*′-tetraacetate acetoxymethyl ester; BHQ, 2,5-di-*tert*-butyl-1,4-benzohydroquinone; BiP, binding immunoglobulin protein; $[Ca^{2+}]_{Cyt}$, cytosolic $[Ca^{2+}]$; $[Ca^{2+}]_{ER}$, endoplasmic reticulum $[Ca^{2+}]$; CAD, CRAC activation domain; CRAC, Ca^{2+}-release activated Ca^{2+} current; ER, endoplasmic reticulum; PM, plasma membrane; SAM, sterile α motif; SERCA, sarcoendoplasmic reticulum Ca^{2+}-ATPase; STIM, stromal interaction molecule; TG, thapsigargin; TIRF, total internal reflection fluorescence.

interactions between the two coiled-coils of its cytosolic tail, the membrane-proximal first coiled-coil acting as an autoinhibitory domain that masks the CAD/STIM-Orai activating region domain and prevents its interaction with Orai channels (23, 24). When cells are stimulated with Ca^{2+}-mobilizing agonists, the decrease in $[Ca^{2+}]_{ER}$ causes Ca^{2+} to dissociate from the STIM luminal EF-hand, and the resulting conformational change promotes the formation of high order STIM oligomers (16) and their translocation toward the plasma membrane. The STIM oligomers accumulate in ER regions juxtaposed to the plasma membrane (25, 26), where they overlap with Orai1 clusters and Ca^{2+} entry sites (27, 28). The ER structures induced by STIM1 appear on the electron microscope as thin ER sheets devoid of chaperones that are still connected to the conventional ER, and we termed these specialized ER compartments "cortical ER" because of their proximity to the PM (29).

Two lines of evidence indicate that the Ca^{2+}-dependent oligomerization of STIM1 is the rate-limiting event in the activation of SOCE. First, the enforced heterodimerization of STIM1 chimeras bearing luminal rapamycin-binding motifs induces STIM1 translocation and Orai1 activation in the absence of Ca^{2+} store depletion, indicating that the oligomerization of STIM1 is sufficient to initiate the cascade of events leading to the activation of plasma membrane channels (30). Second, a point mutation in the STIM1 EF-hand domain that impairs Ca^{2+} binding leads to constitutively SOCE activation, indicating that $[Ca^{2+}]_{ER}$ detection is a crucial step for STIM1 function (12, 31). A $[Ca^{2+}]_{ER}$ value of 169 μM was calculated for half-maximal SOCE activation *in situ*, by measuring the steady-state $[Ca^{2+}]_{ER}$ and the corresponding CRAC currents in cells exposed to different concentrations of the sarco/endoplasmic reticulum Ca^{2+}-ATPase (SERCA) inhibitor cyclopiazonic acid (30). A comparable $[Ca^{2+}]_{ER}$ value (193 μM) was obtained for half-maximal STIM1 oligomerization, measured by fluorescence resonance energy transfer (FRET) between STIM1 fusion proteins, during application of histamine to endothelial cells (32). Interestingly, in this study a lower $[Ca^{2+}]_{ER}$ value was required for half-maximal STIM1 de-oligomerization during store refilling, suggesting that the dissociation process has a higher sensitivity to $[Ca^{2+}]_{ER}$ than the oligomerization process.

The molecular and cellular mechanisms that control SOCE activation have been characterized in details, but the mechanisms that control the retrieval of STIM1 from the plasma membrane and the deactivation of SOCE channels have been comparatively less studied. The oligomerization of STIM is a reversible event (28), and store replenishment is accompanied by STIM1 dissociation from puncta and by its redistribution to deeper ER regions. By analogy with the mechanism of STIM1 activation, it is assumed that Ca^{2+} replenishment of the ER controls the termination of SOCE by inducing the de-oligomerization of STIM1 molecules and their dissociation from the SOCE complex. However, previous studies did not verify that the binding of Ca^{2+} to the EF-hand domain of STIM1 is sufficient to induce the de-oligomerization of STIM1 molecules, their dissociation from the active SOCE complex, and the termination of SOCE. Thus, we do not know whether STIM1 oligomerization and de-oligomerization *in vivo* are exclusively controlled by changes in the ER Ca^{2+} concentration, as inferred from *in vitro* studies.

In this study, we correlate $[Ca^{2+}]_{ER}$ to the extent of STIM1 oligomerization during Ca^{2+} depletion and refilling of the ER in cells treated with agonists or reversible SERCA inhibitors. To manipulate $[Ca^{2+}]_{ER}$ without altering the Ca^{2+} concentration in other cellular compartments, we devised a procedure to refill ER Ca^{2+} stores without adding exogenous Ca^{2+}, using a membrane-permeable Ca^{2+} chelator that provides a large reservoir of buffered Ca^{2+} in the cytoplasm. Our data indicate that although the degree of STIM1 oligomerization exclusively depends on $[Ca^{2+}]_{ER}$, an increase in $[Ca^{2+}]_{ER}$ is not sufficient to induce STIM1 de-oligomerization. In addition to ER Ca^{2+} refilling, a localized cytosolic Ca^{2+} elevation is required for the dissociation of STIM1 complexes and their retrieval from the plasma membrane.

EXPERIMENTAL PROCEDURES

Chemicals—Thapsigargin, histamine, gadolinium, SK&F 96365, ionomycin, and digitonin were purchased from Sigma. 2,5-Di-*tert*-butyl-1,4-benzohydroquinone (BHQ) was purchased from Aldrich Calbiochem. Lanthanum chloride, potassium dihydrogen phosphate, carbonyl cyanide *m*-chlorophenylhydrazone, and sulfinpyrazone were purchased from Fluka. Fura-2/AM and BAPTA-AM were purchased from Molecule Probes Europe (Leiden, The Netherlands). Quest Fluo-8/AM was purchased from AAT Bioquest. $D1_{ER}$ was kindly provided by Drs. Amy Palmer and Roger Tsien (University of California, San Diego, CA).

Plasmids—Human STIM1 cDNA was from OriGene. YFP-STIM1 was a gift from Dr. A. B. Parekh (University of Oxford, United Kingdom). mCherry-STIM1 was a gift from Dr. R. S. Lewis (Stanford University). For CFP-STIM1 construction, CFP was cloned by PCR from $D1_{ER}$ using the primers: forward, 5′-GAG AAC CGG TCG TGA GCA AGG GCG-3′ and reverse, 5′-GCA CGC TGC CGT CCT CGA TGT TGT G-3′. STIM1 was cloned using the primers: forward, 5′-CAC AAC ATC GAG GAC GGC AGC GTG C-3′ and reverse, 5′-GGG GGA ATT CCT ACT TCT TAA GAG GCT TCT TAA AG-3′. Full-length CFP-STIM1 were amplified by recombinant PCR, and cloned into the same vector as YFP-STIM1 between AgeI and EcoRI sites.

Cell Culture and Transfection—HeLa cells were maintained at 37 °C in 5% CO_2 in minimal essential medium containing 10% FCS, 10 μg/ml of streptomycin, and 10 units/ml of penicillin. Cells were seeded on 25-mm diameter glass coverslips and transfected at 70–80% confluence with Lipofectamine 2000 (Invitrogen) by adding 2 μg of plasmid/coverslip, except for co-transfection of CFP-STIM1 and YFP-STIM1, where 0.75 μg of CFP-STIM1 and 2.25 μg of YFP-STIM1 were used. Cells were imaged 48 h after transfection.

Calcium and FRET Measurements—The extracellular solution used for all experiments contained (in mM): 140 NaCl, 5 KCl, 1 $MgCl_2$, 2 $CaCl_2$, 10 glucose, and 20 Hepes (pH 7.4 with NaOH), with $CaCl_2$ replaced by 1 mM EGTA for Ca^{2+}-free solutions. For cytosolic Ca^{2+} measurements, cells were loaded with 2 μM Fura-2/AM for 30 min at room temperature, washed twice, and kept 10–15 min to allow de-esterification. Glass cov-

erslips were inserted in a thermostatic chamber (Harvard Apparatus, Holliston, MA) and experiments were conducted at 37 °C. Cells were imaged using a ×40 oil-immersion objective on an Axiovert microscope (Zeiss) equipped with a 16-bit cooled charge-coupled device camera (MicroMax, Princeton Instruments). Cells were alternatively excited at 340 and 380 nm, using a monochromator (DeltaRam, Photon Technology International Inc.), and emission was collected through a 430DCLP dichroic mirror and a 510WB40 emission filter (Omega Optical, USA). For $[Ca^{2+}]_{ER}$ measurements, cells were transiently transfected with the cameleon probe targeted to the ER ($D1_{ER}$). The oligomerization/de-oligomerization of STIM1 was followed by measuring the FRET signal between CFP- and YFP-STIM1. For $D1_{ER}$ or FRET recordings, cells were excited at 430 nm through a 455-nm dichroic mirror (455DRLP, Omega Optical), and emission was collected alternatively at 480 and 535 nm (480AF30 and 535DF25, Omega Optical) using a filter wheel (Ludl Electronic Products). *In situ* calibration of the $D1_{ER}$ was performed in medium containing (in mM): 10 NaCl, 135 KCl, 1 $MgCl_2$, 20 sucrose, 20 Hepes, 0.01 digitonin, 0.01 ionomycin, 0.005 carbonyl cyanide *p*-chlorophenylhydrazone (pH 7.1 with NaOH). 5 mM EGTA and 5 mM HEDTA were used to buffer free $[Ca^{2+}]$ below 100 μM, and 10 mM HEDTA to buffer free $[Ca^{2+}]$ between 100 μM and 1 mM (Max Chelator Winmaxc version 2.51). To establish the apparent Ca^{2+} dependence of STIM1 oligo/de-oligomerization, STIM1-FRET and $D1_{ER}$ responses obtained in parallel experiments were aligned according to the time of drug application, and FRET change *versus* $[Ca^{2+}]_{ER}$ was fitted using a sigmoid function. For experiments using cytosolic Ca^{2+} buffer, cells were incubated with 20 μM BAPTA-AM for 30 min prior to the measurements. Confocal images (Figs. 1–3) were acquired on an Axiovert 200M (Zeiss) using a spinning wheel disk (Nipkow disc; QLC-100, Visitech Int., UK) with a ×63 oil-immersion objective, and collected by a CCD camera (Photometrics). For cameleon or FRET measurements, cells were excited with a 440 nm diode-pumped solid-state (DPSS) laser line (Coherent), and emission fluorescence was collected simultaneously at 480 and 535 nm using a 450-nm dichroic mirror and a 505 dcxr-D480/30m-D535/40m beam splitter. Image acquisition and processing were done with MetaFluor (version 6.1; Molecular Devices). All the images were background corrected and ratios were divided by the mean ratio recorded during the initial 2 min to minimize the variability between cells (R/R_o).

Rapid Ca^{2+} Imaging—Ca^{2+} microdomain images were acquired using a ×60 oil objective (CFI Plan Apo) of a Nikon A1 microscope (Nikon Instruments, Japan) with the Perfect focus system and equipped with a PMT detector. Prior to the experiment, cells expressing mCherry-STIM1 were incubated with standard solution containing 20 μM BAPTA-AM, 4 μM Fluo-8/AM, and 0.25 mM sulfinpyrazone for 30 min at room temperature. Cells were excited at 488 and 561 nm of a LU4 4-laser unit, and the emission was collected through a 405/488/561/638 dichroic mirror, 525/50 and 595/50 filters. The acquisition was controlled by NIS-Elements software (Nikon).

TIRF Imaging—TIRF (total internal reflection fluorescence) images were obtained on an Axiovert microscope (100M, Zeiss) equipped with a combined epifluorescence/TIRF adapter (TILL Photonics, Germany) using a ×100 oil immersion objective. Cells expressing GFP-STIM1 were excited at 488 nm of a 50 milliwatt tunable laser (Sapphire LP, Coherent) and the emission was collected by a 12-bit CCD camera (Orca 4742-95-ER, Hamamatsu Photonics). Acquisition of images was conducted with Openlab software (version 3.1.7, PerkinElmer Life Sciences).

Statistics—Mean ± S.E. are shown with significance of differences determined by two-tailed Student's *t* test for unpaired samples. $p < 0.05$ was considered to be significant.

RESULTS

$[Ca^{2+}]_{ER}$ Dependence of STIM1 Oligomerization—Several studies have shown that the formation of STIM1 higher order oligomers is the initial step in the signaling cascade that couples ER Ca^{2+} store depletion to SOCE activation (16, 30, 33), but whether the reversible SOCE process is solely controlled by changes in $[Ca^{2+}]_{ER}$ is not known. To address this question, we correlated the changes in free luminal ER Ca^{2+} concentrations ($[Ca^{2+}]_{ER}$) to the extent of STIM1 oligomerization in HeLa cells treated with SERCA pump inhibitors or with Ca^{2+} mobilizing agonists to irreversibly or reversibly deplete their ER Ca^{2+} stores. The degree of STIM1 oligomerization was quantified as the increase in FRET signal in cells coexpressing CFP-STIM1 and YFP-STIM1 (Fig. 1*A*, *upper panel*), and $[Ca^{2+}]_{ER}$ changes were measured in parallel experiments with the ER-targeted cameleon probe $D1_{ER}$ (Fig. 1*A*, *lower panel*). Fig. 1*A* shows the parallel changes in $[Ca^{2+}]_{ER}$ and in FRET, aligned to the time of drug addition, during irreversible depletion of ER Ca^{2+} stores with the SERCA pump inhibitor thapsigargin (TG). *In situ* calibration of the $D1_{ER}$ probe in cells equilibrated at fixed $[Ca^{2+}]_{ER}$ concentrations with ionophores confirmed that the $D1_{ER}$ F_{535}/F_{480} ratio fluorescence increased linearly with $[Ca^{2+}]_{ER}$ over a wide range of Ca^{2+} concentrations (Fig. 1*B*), and enabled to convert the $D1_{ER}$ ratio values to $[Ca^{2+}]_{ER}$. This enabled us to express the STIM1 FRET change as a function of the Ca^{2+} concentration within the ER lumen (Fig. 1*C*). A sigmoid fit of the FRET-$[Ca^{2+}]_{ER}$ relationship obtained during irreversible store depletion with TG yielded an apparent $[Ca^{2+}]_{ER}$ dependence of 306 ± 10.2 μM for the oligomerization of STIM1 (Fig. 1*C*, *dotted line*).

During the oligomerization process, STIM1 molecules are recruited to subplasmalemmal cortical ER domains where they bind and activate Orai1 channels (12, 17, 19, 20, 31). As a result of this translocation, different confocal cellular sections can be either enriched or depleted of STIM1 molecules during store depletion, depending on their proximity to the plasma membrane. To test whether the choice of the confocal plane affected our FRET signal, we compared the responses obtained by imaging a cellular section encompassing the nucleus to the responses obtained by imaging a TIRF-like plane at the cell-substrate interface. Upon TG addition, the fluorescence of both CFP-STIM1 and YFP-STIM1 decayed in the trans-nuclear plane (supplemental Fig. S1*A*), whereas in the near membrane plane the YFP-STIM1 signal increased and the CFP-STIM1 signal slightly was decreased (supplemental Fig. S1*B*). Despite the opposite changes in fluorescence intensities, the changes in the FRET ratio had identical kinetics when measured at the cell

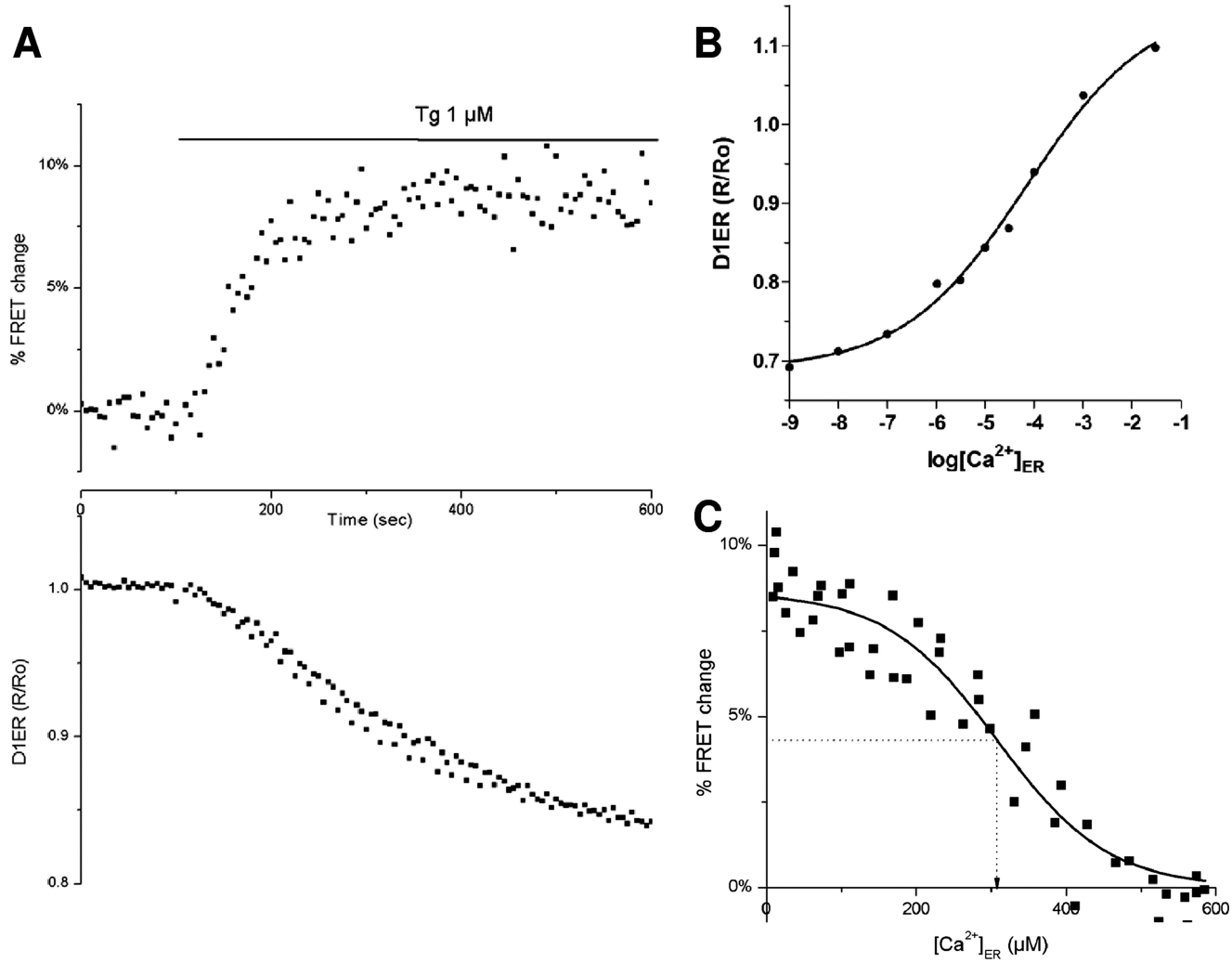

FIGURE 1. **Apparent $[Ca^{2+}]_{ER}$ dependence of STIM1 oligomerization.** *A*, changes in FRET signal between CFP-STIM1 and YFP-STIM1 (*upper panel*) and in $D1_{ER}$ ratio fluorescence (*lower panel*) were measured by confocal microscopy in HeLa cells exposed to 1 μM TG to induce store depletion. Traces are average of 43 and 53 FRET and $D1_{ER}$ recordings, respectively. *B*, *in situ* Ca^{2+} calibration of the $D1_{ER}$ probe in HeLa cells ($n = 33–90$). *C*, apparent $[Ca^{2+}]_{ER}$ dependence of STIM1 oligomerization ($K_d = 306$ μM) induced by TG, established after converting the $D1_{ER}$ ratio values to $[Ca^{2+}]_{ER}$.

center or near the plasma membrane (supplemental Fig. S1*C*). These experiments confirm that the fluorescent STIM1 molecules are recruited to the plasma membrane, and indicate that translocation of STIM1 does not perturb the FRET signal. The FRET changes exhibited a higher dynamics at the plasma membrane (supplemental Fig. S1*B*), but the transnuclear plane was less prone to motion artifacts during long-term recordings and was therefore selected for all subsequent confocal FRET recordings.

To test whether the Ca^{2+} dependence of STIM1 oligomerization varies depending on the speed of the ER depletion, we treated cells with BHQ, a slow-acting SERCA inhibitor, and with histamine, an IP_3-generating agonist that rapidly releases Ca^{2+} from stores. As shown in Fig. 2*A*, BHQ induced a slower and less extensive decrease in $[Ca^{2+}]_{ER}$ than TG, whereas histamine, applied in Ca^{2+}-free medium to maximize store depletion, decreased $[Ca^{2+}]_{ER}$ more rapidly than TG (Fig. 2*A*, *bottom panel*). The different $[Ca^{2+}]_{ER}$ kinetics were mirrored by the kinetics of the FRET change between CFP-STIM1 and YFP-STIM1 (Fig. 2*A*, *top panel*). Interestingly, although the three compounds depleted the stores to different levels (Fig. 2*B*, *lower panel*), the maximal amplitude of the FRET increase was similar (Fig. 2*B*, *upper panel*). As shown in Fig. 2*C*, the FRET-$[Ca^{2+}]_{ER}$ relationships of cells treated with TG and BHQ were similar and overlapped with the FRET-$[Ca^{2+}]_{ER}$ relationship of cells exposed to histamine, which had a steeper slope. These data indicate that the $[Ca^{2+}]_{ER}$ dependence of STIM1 oligomerization is not related to the speed of ER depletion and is largely independent of the stimulus used to deplete the ER.

$[Ca^{2+}]_{ER}$ Dependence of STIM1 De-oligomerization—Having established the $[Ca^{2+}]_{ER}$ dependence of STIM1 oligomerization, we took advantage of the reversibility of histamine and BHQ to study the Ca^{2+} dependence of STIM1 de-oligomerization. For this, cells were exposed to histamine or BHQ in Ca^{2+}-free medium to decrease $[Ca^{2+}]_{ER}$ and increase STIM1 FRET levels, and the drugs were then washed off with a saline solution containing 2 mM Ca^{2+} to promote store refilling. As shown in Fig. 3*A*, Ca^{2+} readmission to cells depleted with BHQ led to a rapid ER refilling and a concomitant decrease in the STIM1 FRET signal. More rapid $[Ca^{2+}]_{ER}$ and FRET responses were

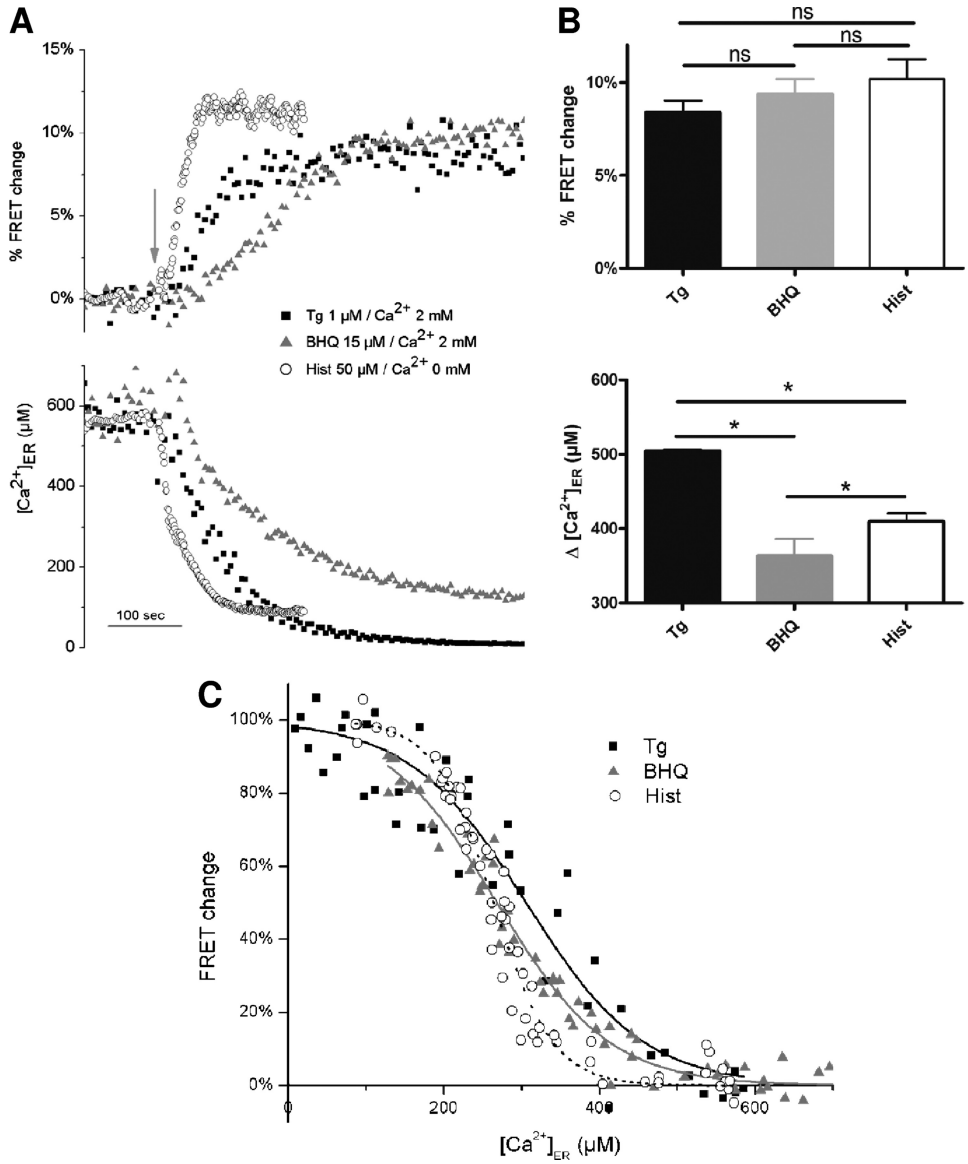

FIGURE 2. **$[Ca^{2+}]_{ER}$ dependence of STIM1 oligomerization during rapid and slow store depletion.** *A*, *upper panel*, average FRET responses evoked by 1 μM TG (*black squares*, $n = 43$), 15 μM BHQ (*gray triangles*, $n = 21$), and 50 μM histamine (*light gray circles*, $n = 27$), applied in Ca^{2+}-containing (TG and BHQ) or Ca^{2+}-free medium (histamine). *Lower panel*, average $D1_{ER}$ responses evoked by TG ($n = 53$), BHQ ($n = 18$), and histamine ($n = 40$). Note the different time courses of FRET increase and store depletion. *B*, statistical evaluation of the FRET (*upper panel*) and $[Ca^{2+}]_{ER}$ (*lower panel*) changes evoked by TG, BHQ, and histamine. The amplitude of the FRET increase was comparable but the three agents decreased by $[Ca^{2+}]_{ER}$ to different extents. *C*, apparent $[Ca^{2+}]_{ER}$ dependence of STIM1 oligomerization evoked by the three protocols of store depletion. TG data are from Fig. 1.

observed when histamine was used to transiently deplete the stores (supplemental Fig. S2). As shown in Fig. 3*B*, the FRET-$[Ca^{2+}]_{ER}$ relationships of the ER refilling phase were similar in cells exposed to the agonist or the SERCA inhibitor (K_d: 152 ± 6.6 and 172 ± 5.5 μM for histamine and BHQ, respectively). This suggests that the $[Ca^{2+}]_{ER}$ dependence of STIM1 de-oligomerization does not depend on the type of stimulus used to deplete the stores. To verify that the $[Ca^{2+}]_{ER}$ dependence of STIM1 de-oligomerization did not vary with the speed of ER refilling, we increased the extracellular Ca^{2+} concentrations from 2 to 20 mM to facilitate the entry of Ca^{2+} into cells. Readmission of 20 mM Ca^{2+} to cells depleted with histamine caused a more extensive decline in the STIM1 FRET signal than readmission of 2 mM Ca^{2+}, the FRET signal decreasing below basal levels (supplemental Fig. S2). However, the FRET-$[Ca^{2+}]_{ER}$ relationships obtained at low and high external Ca^{2+} were nearly identical (K_d: 152 ± 6.6 and 177 ± 2.3 μM for 2 and 20 mM, respectively; Fig. 3*C*). Altogether, these data indicate that $[Ca^{2+}]_{ER}$ dependence of STIM1 de-oligomerization does not depend on the speed of ER replenishment.

Because the FRET-$[Ca^{2+}]_{ER}$ relationships appeared to be independent on the stimulus used, we aggregated all the data collected during store depletion and refilling to better compare the $[Ca^{2+}]_{ER}$ dependence of the oligomerization and de-oligomerization of STIM1. Fig. 3*D* shows the aggregate data obtained under various store depletion conditions (*filled circles*: 1 μM TG or 15 μM BHQ in Ca^{2+} containing medium; 15 μM BHQ or 50 μM histamine in Ca^{2+}-free medium) and store refilling conditions (*open circles*: readmission of 2 or 20 mM Ca^{2+} following histamine or BHQ exposure). The results highlight

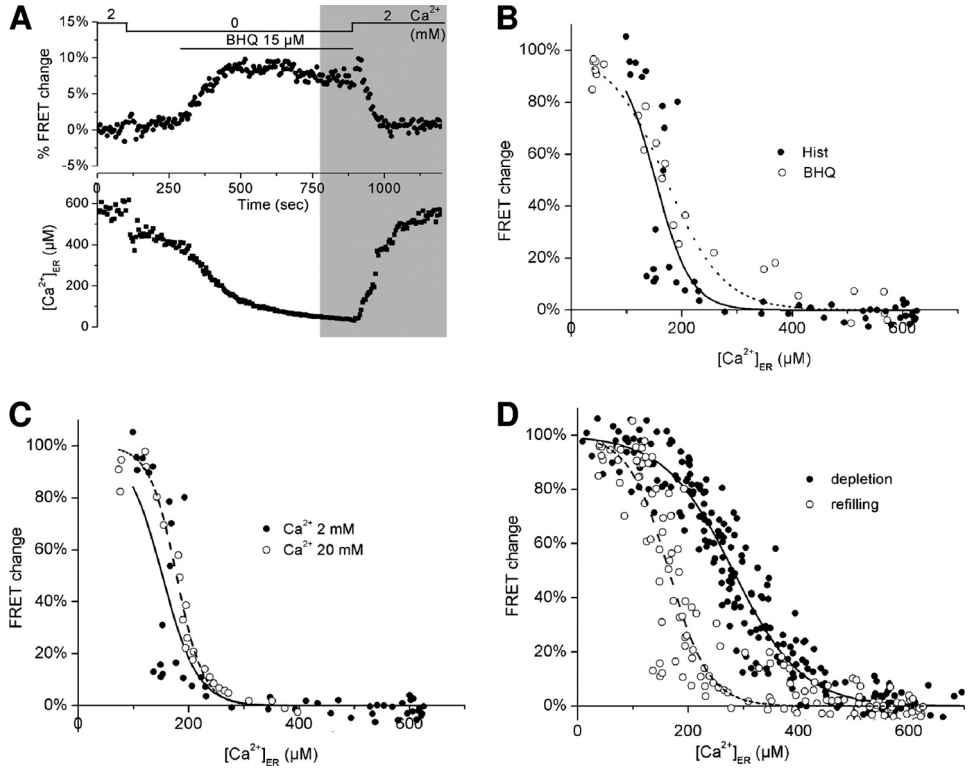

FIGURE 3. **Apparent $[Ca^{2+}]_{ER}$ dependence of STIM1 de-oligomerization.** *A*, *upper panel*, average FRET response ($n = 12$) during transient application of the reversible SERCA inhibitor BHQ (15 μM), removed in Ca^{2+}-containing medium to promote stores refilling. *Lower panel*, average D1ER response ($n = 10$) evoked by this protocol. *B*, $[Ca^{2+}]_{ER}$-FRET relationship during Ca^{2+} readmission to cells depleted with BHQ (*closed circles*) or histamine (*open circles*, $n = 15–22$). *C*, $[Ca^{2+}]_{ER}$-FRET relationship during readmission of 2 mM Ca^{2+} (*closed circles*, $n = 15–22$) or 20 mM Ca^{2+} (*open circles*, $n = 12–18$) to cells depleted with histamine. Data at 2 mM are reported from *panel B*. *D*, aggregate data of all the $[Ca^{2+}]_{ER}$-FRET relationships shown in Fig. 2 (depletion) and this figure (refilling), showing that STIM1 de-oligomerization occurs at lower $[Ca^{2+}]_{ER}$ than oligomerization.

the different $[Ca^{2+}]_{ER}$ dependence of the STIM1 oligomerization and de-oligomerization processes previously reported in endothelial cells (32) and confirm that during store refilling STIM1 de-oligomerizes at lower $[Ca^{2+}]_{ER}$ levels than those required for STIM1 oligomerization (K_d, 281 ± 2.6 and 165 ± 3.2 μM for depletion and refilling, respectively; Fig. 3*D*).

ER Calcium Replenishment Is Not Sufficient to Induce STIM1 De-oligomerization—The left-shifted $[Ca^{2+}]_{ER}$ dependence of STIM1 de-oligomerization could reflect a higher sensitivity of the STIM1 dissociation process to changes in luminal Ca^{2+}, or the presence of additional factors promoting de-oligomerization during store refilling. Elevations in cytosolic Ca^{2+} have been shown to prevent the recruitment of STIM1 to the plasma membrane (32), and might therefore increase the STIM1 de-oligomerization process. $[Ca^{2+}]_{Cyt}$ elevations are unavoidable during store refilling, because the Ca^{2+} ions flowing across SOCE channels must enter the cytosol to be taken up by SERCA. To minimize the cytosolic Ca^{2+} elevations and promote ER refilling in the absence of Ca^{2+} readmission, we loaded cells with BAPTA-AM, a membrane-permeable Ca^{2+} chelator that accumulates inside cells and provides a large reservoir of buffered Ca^{2+} in the cytoplasm (34, 35). Predictably, loading the cells with BAPTA-AM prevented the cytosolic Ca^{2+} elevations evoked by our Ca^{2+} depletion and readmission protocol (supplemental Fig. 2*A*), indicating that cytosolic Ca^{2+} was effectively buffered. To test whether the exogenous Ca^{2+} buffer could provide sufficient Ca^{2+} for ER store refilling, we transiently exposed cells to the reversible inhibitor BHQ in the absence of external Ca^{2+}. As shown in Fig. 4*A*, BHQ removal led to a rapid and complete refilling of the stores in BAPTA-loaded cells (*gray trace*, **2*). In contrast, in cells not exposed to BAPTA the stores remained depleted upon BHQ removal and only refilled upon readmission of external Ca^{2+} (*black trace*, **3*). Statistical evaluation confirmed that BAPTA loading increased $[Ca^{2+}]_{ER}$ as efficiently as Ca^{2+} readmission (Fig. 4*B*, **2* and **3*). These data indicate that, as expected, the SERCA pumps were able to refill the store by extracting the Ca^{2+} buffered by the cytosolic Ca^{2+} chelator. Therefore, this protocol enabled us to test whether ER Ca^{2+} refilling alone, in the absence of external Ca^{2+} readmission, was sufficient to induce STIM de-oligomerization. Strikingly, despite the complete replenishment of the ER in BATPA-loaded cells, the FRET signal between STIM1 molecules remained elevated, suggesting that STIM1 stayed oligomerized (Fig. 4, *C* and *D*, **2*). Subsequent readmission of Ca^{2+} evoked a rapid decrease in the FRET signal, whose kinetics and amplitude were undistinguishable from the decrease observed in control cells (Fig. 4, *C* and *D*, **3*). The increased STIM1 FRET signal of cells with BAPTA-refilled stores might reflect the persistence of oligomerized STIM1 at the cortical ER or the failure of STIM1 to de-oligomerize during its retrieval from the cortical ER. To distinguish between these two possibilities, we followed the formation and disappearance of YFP-STIM1 clusters in cells loaded with BAPTA-AM. As shown in Fig. 4*E*, upon BHQ addition YFP-STIM1 formed visible membrane puncta that persisted upon washout of the inhibitor

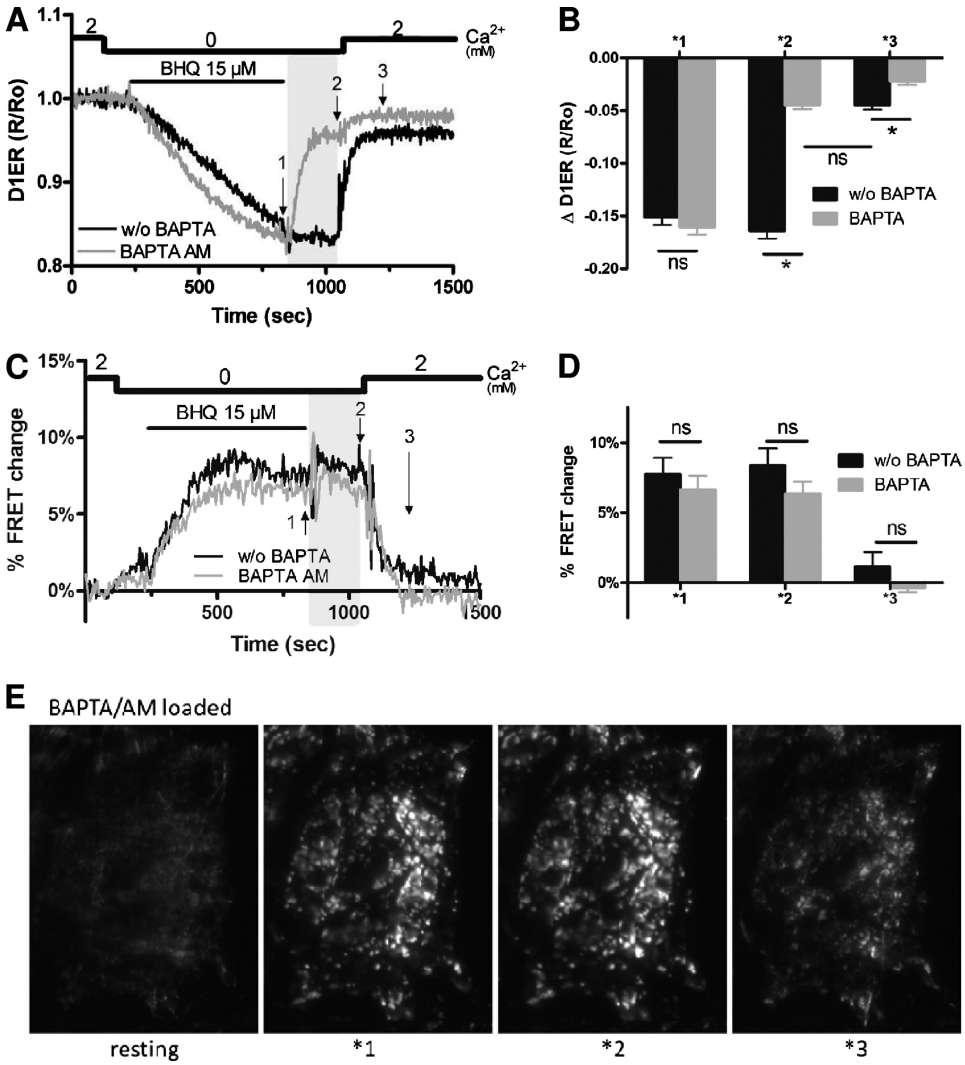

FIGURE 4. **ER refilling does not initiate STIM1 de-oligomerization in BATPA-loaded cells.** Cells were loaded with loaded 20 μM BAPTA-AM to provide a cytosolic reservoir of buffered Ca^{2+} for the refilling of ER Ca^{2+} stores. *A*, average $D1_{ER}$ responses of cells transiently stimulated with BHQ (15 μM) in Ca^{2+}-free medium and subsequently switched to a Ca^{2+}-containing medium. $[Ca^{2+}]_{ER}$ increased immediately upon BHQ removal in BAPTA-loaded cells (*gray traces*, $n = 21$) and only increased upon Ca^{2+} readmission in control cells (*black traces*, $n = 30$). *B*, average decrease in $D1_{ER}$ ratio fluorescence at the time points indicated in *A*; *, $p < 0.001$. Note that $[Ca^{2+}]_{ER}$ increased by the same extent in BAPTA-loaded cells kept in Ca^{2+}-free (*2, BAPTA) than in control cells exposed to 2 mM Ca^{2+} (*3, ctrl). *C*, average FRET responses evoked by the same protocol. The FRET signal remained elevated in BAPTA-loaded cells kept in Ca^{2+}-free cells (*gray traces*, $n = 20$) and decreased upon subsequent readmission of 2 mM Ca^{2+} with kinetics similar to control cells (*black traces*, $n = 20$). *D*, average increase in FRET at the three time points indicated in *A*. *E*, TIRF images of BATPA-loaded cells expressing YFP-STIM1 exposed to the same protocol, taken before stimulation and at the three time points indicated in *A*. Note that the STIM1 puncta persisted after ER refilling (*2) and disappeared upon Ca^{2+} readmission (*3). Images are representative of 4 independent experiments.

(*bottom panel*, *2) and that disappeared upon Ca^{2+} readmission (*3). Thus, in cells loaded with BAPTA, STIM1 remained in cortical ER structures and its de-oligomerization and disappearance from the cortical ER appear to be coordinated events induced by the readmission of Ca^{2+} to cells.

Cytosolic Calcium Is Required for STIM1 De-oligomerization—Having established that the de-oligomerization of STIM1 requires the readmission of Ca^{2+} to cells with refilled stores, we aimed to precise the site of action of this exogenous Ca^{2+}. To test whether Ca^{2+} was acting on an extracellular or intracellular site, we prevented the entry of Ca^{2+} into cells with a maximally effective concentration of La^{3+}, a SOCE channel inhibitor (1). As shown in Fig. 5, *A* and *B*, 50 μM La^{3+} did not affect the $[Ca^{2+}]_{ER}$ increase evoked by BHQ removal in BAPTA-loaded cells (*2, *gray trace*), indicating that the Ca^{2+} trapped by cytosolic BAPTA was efficiently used for ER refilling in the presence of the SOCE inhibitor. In contrast, $[Ca^{2+}]_{ER}$ did not recover when Ca^{2+} was readmitted to control cells in the presence of 50 μM La^{3+} (*3, *black trace*), indicating that SOCE channels were effectively inhibited by La^{3+}. Importantly, the STIM1 FRET signal remained elevated upon Ca^{2+} readmission in both control and BAPTA-loaded cells (Fig. 5, *C* and *D*), indicating that a high extracellular Ca^{2+} concentration is in itself not sufficient to induce STIM1 de-oligomerization. Identical results were obtained with 10 μM Gd^{3+} (Fig. 5, *E* and *F*), whereas BTP2 and SK&F 96365 did not prevent ER refilling upon Ca^{2+} readmission (supplemental Fig. S4) indicating that these two SOCE inhibitors inhibit Ca^{2+} entry less efficiently than La^{3+} and Gd^{3+}. These results strongly suggest that Ca^{2+} is acting from the intracellular, cytosolic side, and therefore that a cytosolic

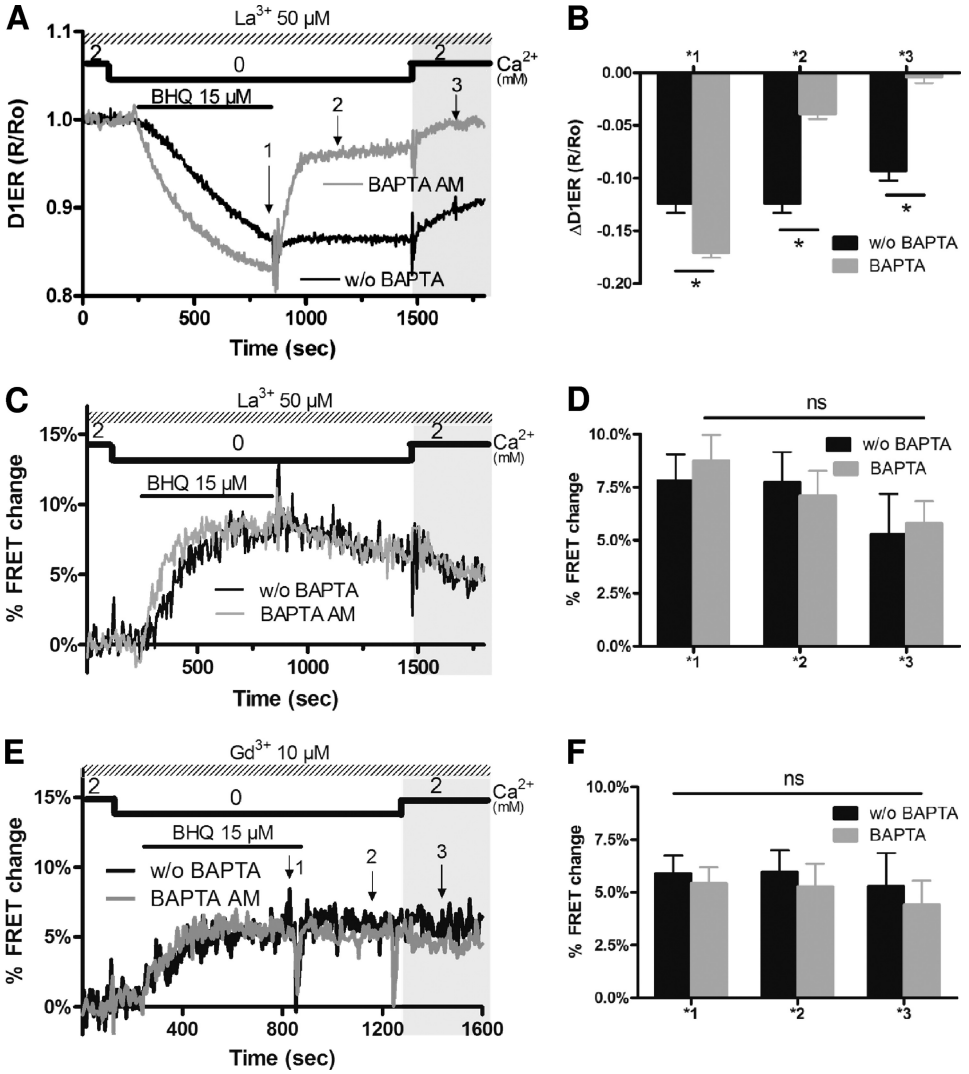

FIGURE 5. **SOCE channel inhibition prevents Ca^{2+}-induced STIM1 de-oligomerization.** Cells were treated as described in the legend to Fig. 4, using bath solutions containing 50 μM La^{3+} (*A–D*) or 10 μM Gd^{3+} (*E* and *F*) to inhibit SOCE channels. *A*, average $D1_{ER}$ responses of control ($n = 36$) and BAPTA-loaded cells ($n = 35$). *B*, average decrease in the $D1_{ER}$ ratio fluorescence at the time points indicated in *A*; *, $p < 0.001$. *C*, average FRET responses evoked by the same protocol. The FRET signal remained elevated during Ca^{2+} readmission to control ($n = 11$) and BATPA-loaded cells ($n = 14$). *D*, average increase in FRET at the three time points indicated in *A*. *E*, average FRET responses recorded with 10 μM Gd^{3+} instead of La^{3+}. The FRET signal remained elevated in both control ($n = 5$) and BATPA-loaded cells ($n = 29$). *F*, average increase in FRET at the three time points indicated in *E*.

Ca^{2+} elevation is necessary to initiate the retrieval of STIM1 from the cortical ER.

To confirm that a localized cytosolic Ca^{2+} elevation occurred during Ca^{2+} readmission to cells loaded with BAPTA, we performed confocal imaging with Fluo-8, a Ca^{2+}-sensitive dye whose fluorescence increases markedly upon Ca^{2+} binding. To localize the Ca^{2+} entry sites, cells were transfected with mCherry-STIM1 and the changes in mCherry and Fluo-8 fluorescence were measured concomitantly during transient depletion of stores with BHQ. As shown in Fig. 6, store depletion induced the apparition of mCherry fluorescence clusters that persisted upon removal of the reversible inhibitor (*top*, *second column*). Ca^{2+} readmission to these BAPTA-loaded cells expressing mCherry-STIM1 evoked localized $[Ca^{2+}]_{Cyt}$ elevations that co-localized with the mCherry fluorescent aggregates but that were of slightly smaller spatial dimension (*bottom*, *third column*). Line scan confocal imaging revealed that the red STIM1 clusters broke apart at the peak of the $[Ca^{2+}]_{Cyt}$ elevations and disappeared entirely shortly after the $[Ca^{2+}]_{Cyt}$ elevations had waned (Fig. 6*B*). Quantification of these images showed that the disappearance of the fluorescent STIM1 clusters correlated with the presence of a local Ca^{2+} elevation (Table 1). Nearly two-thirds of the STIM1 clusters located in the vicinity of a Ca^{2+} hot spot disappeared during the readmission period, whereas the same proportion of STIM1 clusters devoid of Ca^{2+} hot spots remained stable. Due to the small number of STIM1 clusters lacking Ca^{2+} hot spots the relative risk could not be calculated, but the presence of a Ca^{2+} hot spot was associated with an increased probability of STIM1 cluster disappearance (odds ratio: 3.6). These experiments confirm that, in cells loaded with Ca^{2+} chelators, local $[Ca^{2+}]_{Cyt}$ elevations occur at Ca^{2+} entry sites and coincide temporally with the disappearance of STIM1 clusters.

DISCUSSION

In this study, we show that during the activating phase of SOCE, $[Ca^{2+}]_{ER}$ levels are inversely correlated with the degree

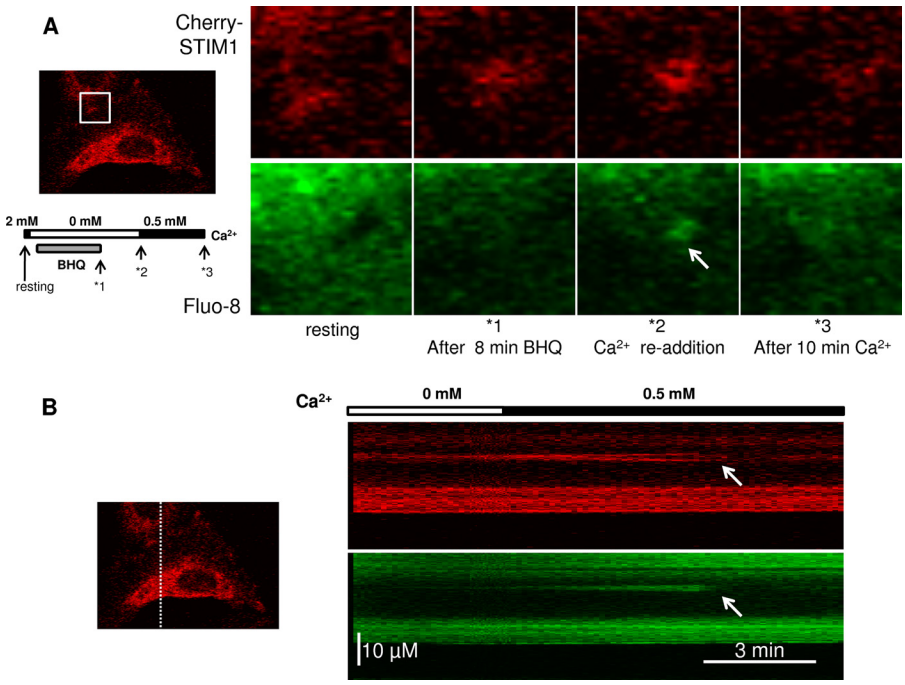

FIGURE 6. **Local cytosolic Ca^{2+} elevations evoked by Ca^{2+} readmission to BATPA-loaded cells.** Cells expressing mCherry-STIM1 were loaded with Fluo-8/AM and BAPTA-AM and imaged by confocal microscopy during transient BHQ application in Ca^{2+}-free and subsequent Ca^{2+} readmission. *A*, mCherry fluorescence (*top*) illustrating the apparition of the STIM1 cluster upon BHQ-induced store depletion and corresponding changes in Fluo-8 fluorescence (*bottom*). Ca^{2+} readmission evoked a local $[Ca^{2+}]_{Cyt}$ elevation that overlapped with the mCherry fluorescence cluster. *B,* line scan confocal image of the mCherry and Fluo-8 fluorescence changes evoked by the readmission of 0.5 mM Ca^{2+}. Distance along the 39-μm scan line is depicted vertically in the image, time runs from *left to right*, and increasing fluorescence intensities (corresponding to increasing free $[Ca^{2+}]_{Cyt}$ for the *bottom panel*) are depicted by increasingly brighter colors. Note that the disappearance of the mCherry fluorescence cluster coincides temporally with the local $[Ca^{2+}]_{Cyt}$ elevation.

TABLE 1

Ca^{2+} hot spots and STIM1 stability

STIM1 clusters shown in Fig. 6 were imaged for 10 min after Ca^{2+} readmission and classified as "stable" or "unstable" if they remained visible or if they had disappeared at the end of the recording. The presence of a Ca^{2+} hot spot in the same spatial domain during the 10-min Ca^{2+} readmission period was then determined to establish the association between Ca^{2+} hot spots and cluster stability. All the Ca^{2+} hot spots were associated with a STIM1 cluster, and no new STIM1 clusters were formed during the readmission period. Two-thirds of the STIM1 clusters associated with a Ca^{2+} hot spot disappeared during the readmission period, whereas two-thirds of the STIM1 clusters lacking Ca^{2+} hot spots remained stable (n = 27 cells from 10 independent recordings, odds ratio: 3.6).

No. of events		STIM1 puncta		
		Stable	Unstable	Total
Ca^{2+} hot spot	Yes	12	26	38
	No	5	3	8
	Total	17	29	46

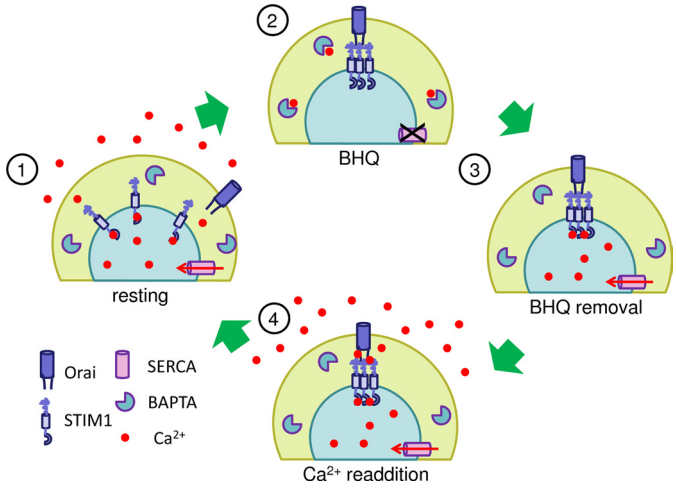

FIGURE 7. **Schematic representation of the STIM1 movement in BAPTA-AM loaded cells.** *1*) at resting $[Ca^{2+}]_{ER}$, STIM1 is in the Ca^{2+}-bound state and evenly distributed on ER membranes. *2*) upon SERCA inhibition, the decrease in $[Ca^{2+}]_{ER}$ induces STIM1 oligomerization and accumulation in PM-associated clusters, where it binds and activates Orai channels. In BAPTA-loaded cells, most of the Ca^{2+} released from the ER is chelated by the cytosolic BAPTA (*blue crescents*) and provides an intracellular reservoir of buffered Ca^{2+}. *3*) relief of SERCA inhibition enables ER refilling as SERCA extract the Ca^{2+} bound to the cytosolic BAPTA, but the restoration of resting $[Ca^{2+}]_{ER}$ levels does not trigger STIM1 de-oligomerization. *4*) upon Ca^{2+} re-admission a local cytosolic Ca^{2+} elevation triggers the de-oligomerization of STIM1 and its retrieval from PM-associated clusters.

of STIM1 oligomerization irrespective of the kinetics of store depletion evoked by agonists or SERCA inhibitors. In sharp contrast, an increase in $[Ca^{2+}]_{ER}$ was not sufficient to initiate STIM1 de-oligomerization, which required a local elevation of the cytosolic Ca^{2+} concentration (Fig. 7).

Previous studies have shown that the extent of SOCE activation is inversely related to $[Ca^{2+}]_{ER}$ levels (30, 32). Accordingly, we observed a strict inverse correlation between $[Ca^{2+}]_{ER}$ and the degree of STIM1 oligomerization, which increased as soon as $[Ca^{2+}]_{ER}$ decreased below basal levels and reached half-maximum at a $[Ca^{2+}]_{ER}$ of ~280 μM. Lower $[Ca^{2+}]_{ER}$ values (~200 μM) were reported for half-maximal I_{CRAC} current activation in Jurkat T cells (30) and for half-maximal STIM1 oligomerization in endothelial cells (32), but in these two studies the resting $[Ca^{2+}]_{ER}$ levels were also significantly lower (~450 *versus* ~520 μM in our HeLa cells). Our higher $[Ca^{2+}]_{ER}$ values do not appear to reflect the poor sensitivity of the $D1_{ER}$ probe (K_d ~60 μM) at high micromolar Ca^{2+} concentrations, because the calibration curve was linear in the pCa range 3–6 (Fig. 1*B*). Despite the discrepancies in absolute $[Ca^{2+}]_{ER}$ values, we also observed that the extent of STIM1 oligomerization was directly propor-

tional to the degree of depletion of ER Ca^{2+} stores, with half-maximal oligomerization occurring when the stores were depleted by 50%. By using agonists or SERCA inhibitors to actively or passively deplete Ca^{2+} stores, we further demonstrate that the $[Ca^{2+}]_{ER}$ dependence of STIM1 oligomerization is independent of the kinetics and mechanisms of ER Ca^{2+} release. More importantly, we show that the $[Ca^{2+}]_{ER}$ dependence of the association and dissociation processes differ markedly, a difference that we could attribute to the need for cytosolic Ca^{2+} elevations to initiate the de-oligomerization process and the disassembly of STIM1 puncta.

The influx of Ca^{2+} across PM channels is both the justification of existence of SOCE and a pre-requisite for its termination, as it provides the ions used for Ca^{2+} replenishment of the ER. The opening of Ca^{2+} permeable channels therefore precedes ER refilling and conveys the signals that subsequently trigger the termination of SOCE. To separate these two intricate processes, we designed a protocol that enables refilling of the ER without adding exogenous Ca^{2+}, thereby bypassing the Ca^{2+} entry phase. We expected that the restoration of a normal ER Ca^{2+} content by the provision of buffered cytosolic Ca^{2+} ions would induce the disaggregation of STIM1 molecules and the disassembly of STIM-Orai1 complexes, because Ca^{2+} binding to STIM1 EF-SAM domains reverse the conformational change induced by the unbinding of Ca^{2+} that leads to STIM1 oligomerization, the key step in the activation process that culminates in the opening of PM channels (30). Early mutagenesis studies showed that Ca^{2+} binding to STIM1 EF-SAM domains stabilizes the molecule in an inactive state (12, 31), whereas subsequent structural studies revealed that the combined EF-SAM domains form a compact structure in the Ca^{2+}-bound state (33) and that Ca^{2+} unbinding leads to a more open configuration that initiates the oligomerization of the luminal domain (16, 36). The reversibility of the conformational changes leading to STIM1 oligomerization suggest that the whole SOCE process is reversibly regulated by Ca^{2+} sensitivity of the luminal STIM domains, and hence by changes in $[Ca^{2+}]_{ER}$ (36). Contrary to this prediction, our experiments in BAPTA-loaded cells showed that the full restoration of normal high $[Ca^{2+}]_{ER}$ levels is not sufficient to initiate the dissociation of STIM1-STIM1 oligomers or the retrieval of STIM1 clusters from the PM (Fig. 7). Despite full replenishment of the ER, the exogenous STIM1 fusion proteins were still associated as evidenced by their high FRET signal, and remained within the same membrane-associated puncta located within a TIRF plane of 100 nm width (Fig. 4). Dissociation was only observed upon readmission of external Ca^{2+} (Fig. 7) and this effect was prevented by the SOC channel blocker La^{3+}, indicating that Ca^{2+} acts on the cytosolic side. In BAPTA-loaded cells, Ca^{2+} readmission did not cause global cytosolic Ca^{2+} elevations (supplemental Fig. S3) but evoked localized Ca^{2+} elevations restricted to STIM1 puncta (Fig. 6). BAPTA loading was used previously to resolve Ca^{2+} entry sites in Jurkat T cells, revealing discrete hot spots of high $[Ca^{2+}]_{Cyt}$ localized in the immediate vicinity of STIM1 puncta (27, 28). Our data now indicate that these highly localized increases in cytosolic Ca^{2+} can trigger the dissociation of STIM1 oligomers and that de-oligomerization of STIM1 occurs coordinately with its retrieval from the plasma membrane. This indicates that the Ca^{2+} ions entering across SOCE channels act on target molecule(s) located in immediate proximity to the STIM1-Orai membrane complexes.

Although local elevation in the cytosolic Ca^{2+} concentration is a pre-requisite for the dissociation of STIM1 oligomers, cytosolic Ca^{2+} elevations are not sufficient to terminate SOCE. It is well known that TG, the drug most commonly used to activate SOCE and study STIM1 translocation, evokes large and long-lasting elevations in cytosolic Ca^{2+} when applied in Ca^{2+}-rich medium (1, 37). Despite persistent $[Ca^{2+}]_{Cyt}$ elevation, treatment with TG induces a massive formation of subplasmalemmal STIM1 clusters and cortical ER (29). Accordingly, STIM1 remained in membrane-associated clusters and the FRET signal did not decrease when Ca^{2+} was readmitted to cells treated with TG, despite a massive global increase in cytosolic Ca^{2+} (data not shown). These data indicate that an increase in $[Ca^{2+}]_{ER}$ is required, but is not sufficient, to terminate SOCE and reverse the conformational changes induced by the unbinding of Ca^{2+} from the STIM1 EF-SAM luminal domain. Our data now show that Ca^{2+} acts not only on the luminal domain of STIM1 but also on a cytosolic target, and that both effects are required for proper termination of SOCE (Fig. 7).

The small size of the local Ca^{2+} elevations occurring in BAPTA-loaded cells indicates that the cytosolic Ca^{2+} targets are likely to be molecules associated with the STIM1-Orai1 complex. CRACR2, a cytosolic Ca^{2+}-binding protein, was reported to stabilize STIM1-Orai1 complexes and dissociate upon Ca^{2+} binding (38), making this molecule a potential target for the Ca^{2+}-dependent inactivation process that we report here. However, the mRNA levels of the two CRACR isoforms were either undetectable (CRACR2A) or very low (CRACR2B) in our HeLa cells, and CRACR2B silencing did not promote STIM1 de-oligomerization during BAPTA-mediated ER refilling (data not shown). Besides CRACR2, SERCA were shown to co-localize with STIM upon store depletion (39, 40) and calmodulin to bind to the polybasic cytosolic tail of STIM1 in a Ca^{2+}-dependent manner (41). The most likely molecular target of the local cytosolic Ca^{2+} elevations, however, is the STIM1 protein itself, because several STIM1 C-terminal domains are involved in productive electrostatic interactions with either the plasma membrane or PM channels. The requirements for exogenous Ca^{2+} persisted in STIM1 mutants lacking the lysine-rich C-terminal domain (data not shown), suggesting that the interactions between the lysine-rich C terminus and membrane phospholipids are not the target of the Ca^{2+} inactivation. Other candidates that remain to be tested include the CRAC modulatory domain (amino acids 474–485), a sequence of seven negatively charged amino acids whose neutralization diminished the fast Ca^{2+}-dependent inactivation of the Orai channel (42). The acidic region was situated on the first coiled-coil domain of STIM, which has an autoinhibitory function by masking the CAD/STIM-Orai activating region domain, and may also contribute to the inactivation of SOCE (23). Finally, the electrostatic interactions between the CAD/STIM-Orai activating region domain and the C terminus of the Orai1 channels might be disrupted by a local elevation in cytosolic Ca^{2+}. Future mutagenesis studies of STIM1 and Orai1 cytosolic domains will

precisely indicate the target of the Ca^{2+} inhibition on the assembled SOCE complex.

One potential caveat of $[Ca^{2+}]_{ER}$ measurements with genetically encoded Ca^{2+} indicators is that the specialized domains derived from the ER that form during SOCE are not accessible to proteins bearing KDEL ER-retention signals. We previously showed that GFP fusion proteins targeted to the ER by virtue of KDEL retention signals do not co-localize with STIM1 and that chaperones such as BiP are excluded from the cortical ER (29). The $D1_{ER}$ probe that we used here to measure $[Ca^{2+}]_{ER}$ contains a KDEL ER retention signal and is also excluded from subplasmalemmal ER regions enriched in STIM1.[3] Despite this limitation, our spatially averaged $D1_{ER}$ measurements likely respond to $[Ca^{2+}]_{ER}$ changes occurring within the cortical ER as this specialized ER compartment is connected with the conventional ER (29). Ca^{2+} moves rapidly within the ER lumen (43, 44), thus the local $[Ca^{2+}]_{ER}$ within the cortical ER is expected to equilibrate with the global $[Ca^{2+}]_{ER}$ of the bulk ER. Given its proximity to the PM, however, the cortical ER might be affected by the Ca^{2+} drag exerted by neighboring plasma-membrane Ca^{2+} pumps, whose function is to extrude Ca^{2+} from cells. During ER refilling with BAPTA, the cortical ER might therefore remain in a depleted condition as plasma-membrane Ca^{2+} pumps compete with SERCA for the extraction of the Ca^{2+} ions bound to the exogenous cytosolic buffer. $[Ca^{2+}]_{ER}$ measurements with a Ca^{2+} probe that can access the cortical ER will be required to clarify this issue.

In a previous study, cytosolic Ca^{2+} elevations were shown to inhibit the formation of subplasmalemmal STIM1 clusters (32). Interestingly, the high Ca^{2+} concentrations had no effects on the kinetics of oligomerization or on the formation of STIM1 aggregates in deep ER regions, but specifically prevented the formation and/or translocation of STIM1 clusters at ER-PM junctions, an effect that was attributed to the reduced velocity of STIM1 comets at high cytosolic Ca^{2+}. The lack of effects of $[Ca^{2+}]_{Cyt}$ on oligomerization are consistent with our observation that $[Ca^{2+}]_{ER}$ dependence of STIM1 oligomerization is similar in cells depleted with agonists or SERCA inhibitors, agents that cause cytosolic Ca^{2+} responses of different amplitude and duration. The inhibitory effects of $[Ca^{2+}]_{Cyt}$ on subplasmalemmal STIM1 clustering does not appear to be a dominant feature of the SOCE process because, as mentioned above, STIM1 forms membrane clusters and is recruited to the cortical ER in cells treated with TG, despite large elevations in cytosolic Ca^{2+}. Our finding that a cytosolic Ca^{2+} elevation is required to induce the de-oligomerization of STIM1 might account for the delayed apparition of new clusters at high $[Ca^{2+}]_{Cyt}$ reported in this study (32). Accordingly, these authors also observed that $[Ca^{2+}]_{Cyt}$ elevations promoted the disassembly of pre-existing STIM1 clusters. The main effect of cytosolic Ca^{2+} elevations is therefore not to inhibit the formation of subplasmalemmal STIM1 clusters but to induce the de-oligomerization of STIM1.

In summary, we show here that the restoration of physiological $[Ca^{2+}]_{ER}$ levels is not sufficient to induce de-oligomerization of STIM1 or the disaggregation of STIM1 membrane clusters, and that both processes require a local increase in cytosolic Ca^{2+} in the vicinity of plasma membrane STIM1 clusters. Ca^{2+} act at two distinct sites on both sides of the ER membrane to control the retrieval of STIM1 from the plasma membrane and the termination of SOCE.

Acknowledgments—We thank Drs. R. Y. Tsien and A. Palmer for providing the cameleon constructs and Cyril Castelbou for expert technical assistance.

[3] N. Demaurex, unpublished observations.

REFERENCES

1. Parekh, A. B., and Putney, J. W., Jr. (2005) *Physiol. Rev.* **85,** 757–810
2. Clapham, D. E. (2007) *Cell* **131,** 1047–1058
3. Feske, S. (2009) *Immunol. Rev.* **231,** 189–209
4. Parekh, A. B. (2010) *Nat. Rev. Drug Discov.* **9,** 399–410
5. Hogan, P. G., Lewis, R. S., and Rao, A. (2010) *Annu. Rev. Immunol.* **28,** 491–533
6. Vig, M., and Kinet, J. P. (2009) *Nat. Immunol.* **10,** 21–27
7. Stiber, J., Hawkins, A., Zhang, Z. S., Wang, S., Burch, J., Graham, V., Ward, C. C., Seth, M., Finch, E., Malouf, N., Williams, R. S., Eu, J. P., and Rosenberg, P. (2008) *Nat. Cell Biol.* **10,** 688–697
8. Darbellay, B., Arnaudeau, S., Konig, S., Jousset, H., Bader, C., Demaurex, N., and Bernheim, L. (2009) *J. Biol. Chem.* **284,** 5370–5380
9. Collins, S. R., and Meyer, T. (2011) *Trends Cell Biol.* **21,** 202–211
10. Putney, J. W., Jr. (1986) *Cell Calcium* **7,** 1–12
11. Roos, J., DiGregorio, P. J., Yeromin, A. V., Ohlsen, K., Lioudyno, M., Zhang, S., Safrina, O., Kozak, J. A., Wagner, S. L., Cahalan, M. D., Veliçelebi, G., and Stauderman, K. A. (2005) *J. Cell Biol.* **169,** 435–445
12. Liou, J., Kim, M. L., Heo, W. D., Jones, J. T., Myers, J. W., Ferrell, J. E., Jr., and Meyer, T. (2005) *Curr. Biol.* **15,** 1235–1241
13. Vig, M., Peinelt, C., Beck, A., Koomoa, D. L., Rabah, D., Koblan-Huberson, M., Kraft, S., Turner, H., Fleig, A., Penner, R., and Kinet, J. P. (2006) *Science* **312,** 1220–1223
14. Zhang, S. L., Yeromin, A. V., Zhang, X. H., Yu, Y., Safrina, O., Penna, A., Roos, J., Stauderman, K. A., and Cahalan, M. D. (2006) *Proc. Natl. Acad. Sci. U.S.A.* **103,** 9357–9362
15. Feske, S., Gwack, Y., Prakriya, M., Srikanth, S., Puppel, S. H., Tanasa, B., Hogan, P. G., Lewis, R. S., Daly, M., and Rao, A. (2006) *Nature* **441,** 179–185
16. Stathopulos, P. B., Li, G. Y., Plevin, M. J., Ames, J. B., and Ikura, M. (2006) *J. Biol. Chem.* **281,** 35855–35862
17. Park, C. Y., Hoover, P. J., Mullins, F. M., Bachhawat, P., Covington, E. D., Raunser, S., Walz, T., Garcia, K. C., Dolmetsch, R. E., and Lewis, R. S. (2009) *Cell* **136,** 876–890
18. Kawasaki, T., Lange, I., and Feske, S. (2009) *Biochem. Biophys. Res. Commun.* **385,** 49–54
19. Yuan, J. P., Zeng, W., Dorwart, M. R., Choi, Y. J., Worley, P. F., and Muallem, S. (2009) *Nat. Cell. Biol.* **11,** 337–343
20. Calloway, N., Holowka, D., and Baird, B. (2010) *Biochemistry* **49,** 1067–1071
21. Muik, M., Fahrner, M., Derler, I., Schindl, R., Bergsmann, J., Frischauf, I., Groschner, K., and Romanin, C. (2009) *J. Biol. Chem.* **284,** 8421–8426
22. Demaurex, N., and Frieden, M. (2003) *Cell Calcium* **34,** 109–119
23. Korzeniowski, M. K., Manjarrés, I. M., Varnai, P., and Balla, T. (2010) *Sci. Signal.* **3,** ra82
24. Wang, Y., Deng, X., and Gill, D. L. (2010) *Sci. Signal.* **3,** pe42
25. Wu, M. M., Buchanan, J., Luik, R. M., and Lewis, R. S. (2006) *J. Cell Biol.* **174,** 803–813
26. Grigoriev, I., Gouveia, S. M., van der Vaart, B., Demmers, J., Smyth, J. T., Honnappa, S., Splinter, D., Steinmetz, M. O., Putney, J. W., Jr., Hoogenraad, C. C., and Akhmanova, A. (2008) *Curr. Biol.* **18,** 177–182
27. Luik, R. M., Wu, M. M., Buchanan, J., and Lewis, R. S. (2006) *J. Cell Biol.* **174,** 815–825
28. Liou, J., Fivaz, M., Inoue, T., and Meyer, T. (2007) *Proc. Natl. Acad. Sci. U.S.A.* **104,** 9301–9306
29. Orci, L., Ravazzola, M., Le Coadic, M., Shen, W. W., Demaurex, N., and

Cosson, P. (2009) *Proc. Natl. Acad. Sci. U.S.A.* **106,** 19358–19362
30. Luik, R. M., Wang, B., Prakriya, M., Wu, M. M., and Lewis, R. S. (2008) *Nature* **454,** 538–542
31. Zhang, S. L., Yu, Y., Roos, J., Kozak, J. A., Deerinck, T. J., Ellisman, M. H., Stauderman, K. A., and Cahalan, M. D. (2005) *Nature* **437,** 902–905
32. Malli, R., Naghdi, S., Romanin, C., and Graier, W. F. (2008) *J. Cell Sci.* **121,** 3133–3139
33. Stathopulos, P. B., Zheng, L., Li, G. Y., Plevin, M. J., and Ikura, M. (2008) *Cell* **135,** 110–122
34. Tsien, R. Y. (1980) *Biochemistry* **19,** 2396–2404
35. Larson, L., Arnaudeau, S., Gibson, B., Li, W., Krause, R., Hao, B., Bamburg, J. R., Lew, D. P., Demaurex, N., and Southwick, F. (2005) *Proc. Natl. Acad. Sci. U.S.A.* **102,** 1921–1926
36. Stathopulos, P. B., and Ikura, M. (2010) *Biochem. Cell Biol.* **88,** 175–183
37. Jousset, H., Frieden, M., and Demaurex, N. (2007) *J. Biol. Chem.* **282,** 11456–11464
38. Srikanth, S., Jung, H. J., Kim, K. D., Souda, P., Whitelegge, J., and Gwack, Y. (2010) *Nat. Cell. Biol.* **12,** 436–446
39. Manjarrés, I. M., Rodríguez-García, A., Alonso, M. T., and García-Sancho, J. (2010) *Cell Calcium* **47,** 412–418
40. Sampieri, A., Zepeda, A., Asanov, A., and Vaca, L. (2009) *Cell Calcium* **45,** 439–446
41. Bauer, M. C., O'Connell, D., Cahill, D. J., and Linse, S. (2008) *Biochemistry* **47,** 6089–6091
42. Derler, I., Fahrner, M., Muik, M., Lackner, B., Schindl, R., Groschner, K., and Romanin, C. (2009) *J. Biol. Chem.* **284,** 24933–24938
43. Mogami, H., Nakano, K., Tepikin, A. V., and Petersen, O. H. (1997) *Cell* **88,** 49–55
44. Park, M. K., Petersen, O. H., and Tepikin, A. V. (2000) *EMBO J.* **19,** 5729–5739